# Imprint of Holocene Climate Variability on Cold-Water Coral Reef Growth at the SW Rockall Trough Margin, NE Atlantic

Lucile Bonneau, Christophe Colin, Edwige Pons-Branchu, Furu Mienis, Nadine Tisnerat-Laborde, Dominique L Blamart, Mary Elliot, Tim Collart, Norbert Frank, Lorna Foliot, et al.

AGU100 ADVANCING EARTH AND SPACE SCIENCE

Geochemistry, Geophysics, Geosystems

RESEARCH ARTICLE
10.1029/2018GC007502

# Imprint of Holocene Climate Variability on Cold-Water Coral Reef Growth at the SW Rockall Trough Margin, NE Atlantic

**Lucile Bonneau[1,2,3], Christophe Colin[2], Edwige Pons-Branchu[1], Furu Mienis[4], Nadine Tisnérat-Laborde[1], Dominique Blamart[1], Mary Elliot[5], Tim Collart[6], Norbert Frank[3], Lorna Foliot[1], and Eric Douville[1]**

[1]Laboratoire des Sciences du Climat et de l'Environnement, LSCE/IPSL, CEA-CNRS-UVSQ, Université Paris-Saclay, Gif-sur-Yvette, France, [2]Laboratoire GEOsciences Paris-Sud (GEOPS), UMR 8148, CNRS-Université de Paris-Sud, Université Paris-Saclay, Orsay, France, [3]Universität Heidelberg, Heidelberg, Germany, [4]Royal Netherlands Institute for Sea Research (NIOZ) and Utrecht University, Den Burg, Netherlands, [5]LPGNantes, Université de Nantes, Nantes, France, [6]Ghent University, Department of Geology, Ghent, Belgium

**Key Points:**
- First detailed record of cold-water corals occurrence at the SW Rockall Trough margin during the Holocene
- Evidence of a mid-Holocene increase in the cold-water corals occurrence associated to major reorganization of the hydrology
- Strong evidence of millennial climatic control on the CWC growth in the SW Rockall Trough during the late-Holocene

**Correspondence to:**
C. Colin,
christophe.colin@u-psud.fr

**Citation:**
Bonneau, L., Colin, C., Pons-Branchu, E., Mienis, F., Tisnérat-Laborde, N., Blamart, D., et al. (2018). Imprint of holocene climate variability on cold-water coral reef growth at the SW Rockall Trough margin, NE Atlantic. *Geochemistry, Geophysics, Geosystems*, *19*, 2437–2452. https://doi.org/10.1029/2018GC007502

Received 22 FEB 2018
Accepted 8 MAY 2018
Accepted article online 25 MAY 2018
Published online 11 AUG 2018

**Abstract** U-Th ages and temperatures derived from Li/Mg have been measured on coral fragments of *Lophelia pertusa* and *Madrepora oculata* collected from two sediment cores, which were taken from cold-water coral (CWC) mounds at 700–790 m water depth at the SW Rockall Trough margin. Our data, combined with previous published data, have allowed us to first estimate the occurrence of CWC at the SW Rockall Trough margin during the Holocene and, second, to better constrain the environmental conditions driving variability in CWC growth. CWC abundance is marked by a pronounced increase in the mid-Holocene (~6 ka) and is modulated by millennial-scale variability throughout the late-Holocene. The mid-Holocene proliferation of CWC coincides with lowest IRD abundances and a major reorganization of the circulation at thermocline depth in the Rockall Trough, marked by the progressive replacement of the fresh-cold Sub-Arctic Intermediate Water (SAIW) by the saltier and nutrient-rich Eastern North Atlantic Water (ENAW). This event must have established a modern-like winter mixed layer and thermocline structure, generating suitable conditions for enhanced surface productivity, downslope transport of food particles, bottom current acceleration at mound depth and thus CWC growth. Several short time intervals of decreased CWC occurrences closely match prominent increases in North Atlantic drift ice and storminess in Northern Europe. We, therefore, propose that high detrital supply and/or changes in the vertical density gradient associated with millennial-scale ice-rafted detritus (IRD) events are the likely controlling factors for CWC growth and subsequent mound formation on the SW Rockall Trough margin.

## 1. Introduction

In the Northeast Atlantic, framework forming CWC predominantly occur along the European continental margin, between ~100 and 1,000 m water depth (e.g., Findlay et al., 2014; Frank et al., 2011; Freiwald et al., 2004, 2016; Mohn et al., 2014; White & Dorschel, 2010). They appear as solitary colonies or coral patches, but at specific sites can also form large reefs and mounds (De Mol et al. 2002; van Weering et al., 2003a). Several physical parameters are known to be important for CWC reef growth in the NE Atlantic, such as temperatures of between 4°C and 12°C, density in the range of 27.35–27.65 kg $m^{-3}$ (De Mol et al., 2011; Dullo et al., 2008; Sánchez et al., 2014; White & Dorschel, 2010), and energetic near-bottom flow dynamics (Findlay et al., 2014; Frederiksen et al., 1992; Freiwald, 2002; Kenyon et al., 2003; Masson et al., 2003; Roberts et al., 2009; White & Dorschel, 2010). Modern spatial distributions of CWC are strongly related to vertical supply of fresh labile organic matter (Davies et al., 2008) and bottom currents that permit coral larvae dispersal and prevent corals from being smothered by sediment (Mienis et al., 2007, 2009; Sánchez et al., 2014; Somoza et al., 2014).

The cluster of coral mounds on the SW Rockall Trough margin, named the Logachev mound after the research vessel R/V Professor Logachev, represents a well-studied hotspot for CWC growth. Carbonate mounds, measuring from several hundred meters to several kilometers in diameter and reaching heights of up to 160 m above the surrounding seafloor, are found in this area (de Haas et al., 2009; Kenyon et al., 2003) at a specific water-depth range (between 600 and 1,000 m water depth). This area is further characterized

by intense near-bottom currents, which are controlled by tidal interaction with the topography (Mohn et al., 2014). Internal waves of up to 120 m amplitude have been observed, which, being 100 times greater than in the open-ocean, increase the turbulence around the mounds. These motions are locally important for food particle supply and residence time and they allow nutrient and oxygen replenishment of the CWC reef and prevent them from being buried beneath sediments (Van Haren et al., 2014). These diurnal oscillations induce movements of the thermocline and are highlighted by daily temperature variations of up to ~3°C at the thermocline depth (Duineveld et al., 2007; Mienis et al., 2007; Van Haren et al., 2014; van Weering et al., 2003b).

U-series dating of fossil CWC fragments retrieved from carbonate mounds have been used to investigate the late-Quaternary spatial and temporal distribution of CWC in the North Atlantic (Dorschel et al., 2005; Douarin et al., 2013; Frank et al., 2009, 2011; Lopez Correa et al., 2012; Lutringer, 2003; Victorero et al., 2016). At high latitudes, between 50°N and 70°N, interglacial climates were favorable for continuous CWC growth and carbonate mound development, while no CWC from glacial periods have been discovered and dated in this region until present (Douarin et al., 2013; Frank et al., 2009, 2011; Schröder-Ritzau et al., 2005; Van der Land et al., 2014). On the contrary, glacial periods are associated with increased framework forming CWC reef growth at temperate latitudes between 20°N and 50°N (Frank et al., 2011; Wienberg et al., 2010). Such glacial-interglacial changes in the North-South distribution of CWC reefs have been linked to the North-South displacement of cold nutrient-rich intermediate waters and surface productivity driven by changes in the position of the polar front (Frank et al., 2011). However, other mechanisms could be involved in the emergence of this pattern, such as changes in the temperature and related pycnocline, which is associated with the development of nepheloid layers (Raddatz et al., 2014; Rüggeberg et al., 2016) or changes in detrital input (e.g., ice-rafted debris) (Pirlet et al., 2011; Thierens et al., 2012).

The formation of an individual coral mound is cyclic depending on the interaction between coral growth (death and decline) and sediment deposition (de Haas et al., 2009). Continuous growth of individual colonies followed by periods of colony decomposition and sedimentation often results in a characteristic stepped age/depth profile in coral bearing sediment cores. Roberts et al. (2009) report that long-term cycles are controlled by environmental conditions (e.g., glacial-interglacial cycles and consequently temperature and carbon cycles), while short-term cyclic growth is probably linked to the internal stability of the individual patches of coral. Therefore, because of these local internal cycles, the development record from a single coral mound is not necessarily representative of the overall temporal and spatial development of all mounds. For the moment, composite records of temporal CWC abundances at mound province-scale are scarce. Several studies have compiled CWC ages along the Western European margin and the Mediterranean Sea in order to try to estimate the larger-scale patterns of decline and growth of CWC reefs under known climate change conditions (Dorschel et al., 2005; Douarin et al., 2013; Fink et al., 2013; Frank et al., 2009, 2011; Lopez Correa et al., 2012; Schröder-Ritzau et al., 2005; Wienberg et al., 2010). One of the most complete composite records, published by Frank et al. (2009), is a compilation of 87 U-Th dated CWC collected from the Rockall Trough and Porcupine Seabight. In this region, CWC have been active since they first appeared almost simultaneously on several mounds at the onset of the Holocene (~11 ka). During the Holocene, Frank et al. (2009) report several stages of coral decline at 1.8–2.0, 4.2–4.8, and 6–8.2 ka which they hypothesized could be related to significant environmental change. However, the reason for such changes remain unknown.

In this study, coral fragments of *Lophelia pertusa* and *Madrepora oculata* were sampled at high-resolution in two additional sediment cores from the SW Rockall Trough margin located at ~750 m water depth. U-Th ages of individual fragments were analyzed and combined with previous results mainly obtained by Frank et al. (2009) for several neighboring mounds in the Logachev mound province (Figure 1). This allows us to better constrain the processes modulating CWC growth at a regional scale. Our strategy is to link growth periods with in situ bottom water temperature estimates derived from Li/Mg ratios in CWC (Montagna et al., 2014), and then to link these results with North Atlantic middepth Ocean circulation proxies in order to assess whether millennial-scale water mass dynamics influence CWC occurrences in the Northeast Atlantic.

## 2. Hydrological Settings and CWC Environment of the SW Rockall Trough

CWC mounds are present on the SW Rockall Trough margin between 600 and 1,000 m water depth (Figure 1; Mienis et al., 2006; van Weering et al., 2003b) corresponding to temperature and salinity ranges of 6.2–

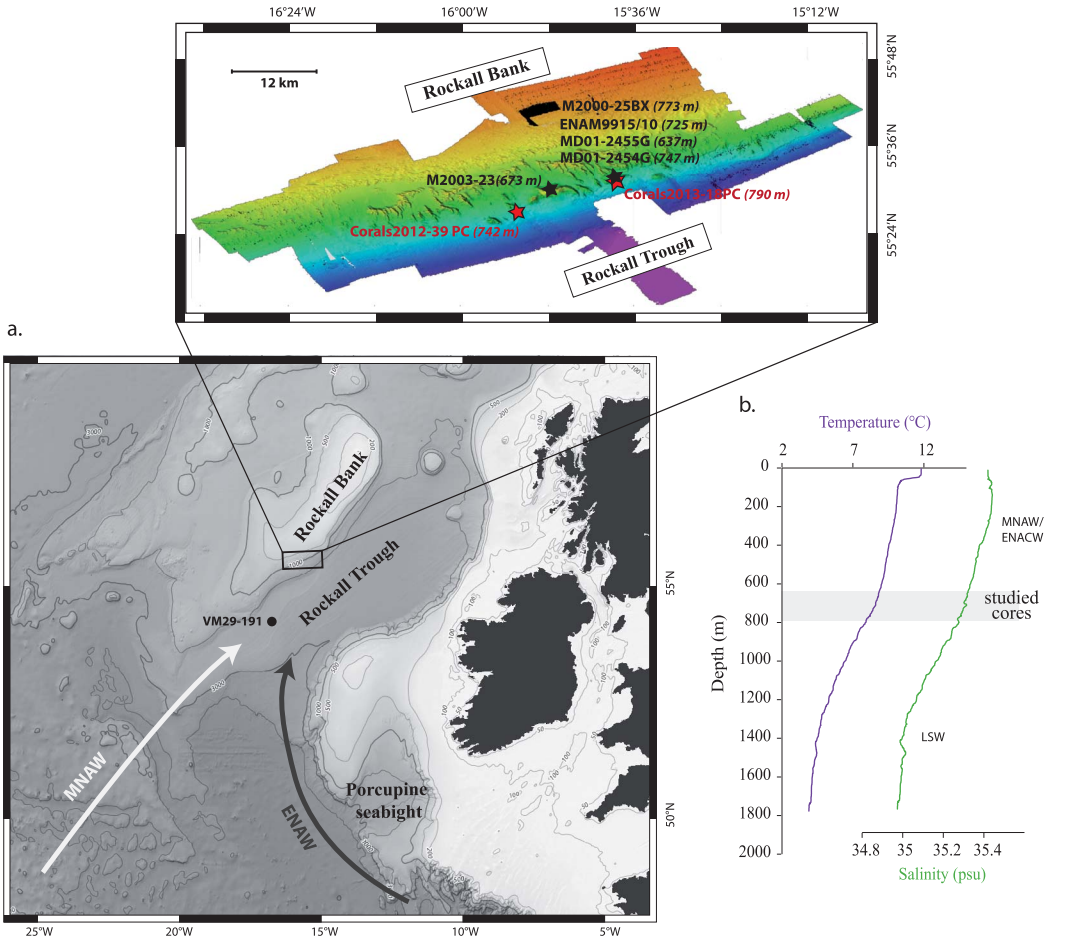


**Figure 1.** (a) Bathymetric map showing the location of the studied cores (Corals2012-39PC, Corals2013-18PC, M2000-25BX, and MD01–2454G) and all other cores discussed in this studied. Core VM29–191 was used to establish the IRD record (Bond et al., 1997). (b) Potential temperature (°C) and salinity depth profiles for the water station ICE-CTD-03 located in the SW Rockall Trough (55°56′N, 14°24′W; 1,750 m; June 2012) close to the studied site (Dubois-Dauphin et al., 2017). The water depth of the modern CWC investigated in this study has been reported by a grey horizontal band. The main water masses present at modern time in the SW Rockall Trough are Modified North Atlantic Water (MNAW), East North Atlantic Central Water (ENACW), and the Labrador Sea Water (LSW).

9.8°C and 35.13–35.4, respectively (Mienis et al., 2007; New & Smythe-Wrigh, 2001). Due to a relatively weak density gradient in the upper layers, the Rockall Trough is marked by wintertime mixing of the near-surface layers reaching a depth of 500–700 m (Ellett & Martin, 1973; Holliday et al., 2000) and up to 1,000 m during severe winters (New & Smythe-Wright, 2001). The resulting upper-layer water mass is a mix of saline Eastern North Atlantic Central Water (ENACW), originating from the Bay of Biscay (Ellett et al., 1986; Ellett & Martin, 1973; Pollard et al., 1996), and fresher Modified North Atlantic Water (MNAW) carried by the North Atlantic Current (NAC) (New & Smythe-Wright, 2001). The MNAW is formed by the mixing of the Western North Atlantic Central Water (WNACW), which flows from the Caribbean Sea with the Sub-Arctic Intermediate Water (SAIW), which is derived from the Labrador current. Most of the water entering into the Rockall Trough at middepth originates from the western European margin and the presence of MNAW in the Rockall Trough is closely linked to the position of the Sub-Polar Gyre (SPG) and the NAO (Bower et al., 2002).

Below the near-surface layer, warm and saline Mediterranean Sea Water (MSW) propagates northward as an eastern boundary undercurrent, typically at depths of 1,000–1,200 m, along the European margin. Lozier and Stewart (2008) have recently shown that the northward penetration of the MSW along the eastern boundary of the North Atlantic is characterized by significant temporal variability in relation to the NAO index and the Sub-Polar Gyre expansion, implying the possibility of short-lived penetration of the MOW into the Rockall Trough. The inflow of Labrador Sea Water (LSW) into the Rockall Trough occurs at water

depths ranging from 1,600 to 1,900 m and is characterized by a marked salinity minimum (New & Smythe-Wright, 2001).

## 3. Materials and Methods

### 3.1. Cold-Water Coral and Foraminifera Samples

Fifty-three CWC samples belonging to the species *L. pertusa* and *M. oculata* were sampled in two sediment cores, Corals2012-39PC (55.452°N–15.870°W, 742 m water depth; length 413 cm, n = 44) and Corals2013-18PC (55.523°N–15.644°W, 790 m water depth; length 397 cm, n = 9), which were collected during cruise 64PE360-Corals2012 and 64PE377-Corals2013, respectively. In addition, one living sample of *L. pertusa* was collected with a box corer (M2000-25BX) in the same area in August 2000 (55.542°N–15.6475°W, 773 m water depth) (Table 1 and Figure 1). The three coring sites, situated at about 16 km apart, are located at the summits of two individual carbonated mounds at the SW Rockall Trough margin (Figure 1 and Table 1). The sediment cores are composed of biogenic fragments (mainly CWC fragments) within a carbonate matrix. The main CWC species found in cores Corals2012-39PC and Corals2013-18PC was *L. pertusa*, however, other Scleractinia of the species *M. oculata* and *Desmophyllum dianthus* were also identified. The base of the Corals2012-39PC core (below 385 cm) is composed of carbonate cement forming a hard-ground. The top of this hard-ground is associated with the occurrence of dropstones and volcanic glass. Such hard-grounds have also been observed in several other cores retrieved from neighboring mounds (i.e., MD01–2454G, M2003-23, and M2001-28) (Figure 1) but were not observed in Corals2013-18PC (Van der Land et al., 2010). $^{230}Th/^{234}U$ dating (n = 53) and Li/Mg temperature determination (n = 43) have been realized on these CWC samples.

In addition, 14 sediments samples have been collected surrounding the CWC fragments in Corals2012-39PC (n = 9) and MD01–2454G (n = 5) for radiocarbon accelerator mass spectrometry (AMS) dating of planktonic foraminifera. Gravity core MD01–2454G (55°31′17N–15°39′08W, 747 m water depth), used in this study for comparison, was retrieved during the R/V Marion Dufresne expedition "MD123" in September 2001 and is located very close to core Corals2013-18PC (Table 1 and Figure 1).

### 3.2. Analytical Procedures

#### 3.2.1. U/Th Dating

CWC samples were analyzed for $^{230}Th/^{234}U$ dating at the Laboratoire des Sciences du Climat et de l'Environnement (LSCE, Gif-sur-Yvette, France). Prior to analysis, the samples were carefully cleaned using a small diamond blade to remove any optically visible contamination (Fe-Mn coatings) and sediment-filled cavities. The fragments were examined under a binocular microscope to eliminate the presence of bioeroded parts and finally the fragments were crushed into a coarse-grained powder using an agate mortar and pestle. The powders (~60–100 mg) were transferred to acid cleaned Teflon beakers, ultrasonicated in MilliQ water, leached with 0.01 N HCl for ~15 s and finally rinsed twice with MilliQ water. The U and Th separation and purification followed a procedure modified from Pons-Branchu et al. (2005) and Douville et al. (2010). The

**Table 1**
*List of Cores Collected in the SW Rockall Bank From Which Dated CWC Were Used in This Study and Corresponding Publications*

| Name | Type | Lat. °N | Long. °W | Depth (m) | Length (cm) | Reference |
|---|---|---|---|---|---|---|
| Corals2012-39PC | Gravity core | 55.452 | 15.870 | 742 | 413 | This study |
| Corals2013-18PC | Gravity core | 55.523 | 15.644 | 790 | 397 | This study |
| M2000-25BX | Box core | 55.542 | 15.6475 | 773 | | This study |
| MD01–2454G | Gravity core | 55.519 | 15.651 | 747 | 273 | Colin et al. (2010)<br>Frank et al. (2009) |
| MD01–2455G | Gravity core | 55.550 | 15.666 | 637 | 193 | Frank et al. (2009) |
| M2003-23 | Piston core | 55.504 | 15.785 | 673 | 440 | Mienis et al. (2009) |
| ENAM-9910 | Box core | 55.533 | 15.666 | 725 | | Frank et al. (2004) |
| ENAM-9915 | Box core | 55.533 | 15.666 | 725 | | Copard et al. (2012)<br>Frank et al. (2004) |

*Note*. See also Figure 1.

physically and chemically cleaned samples were dissolved in 3–4 ml dilute HCl (~10%) and mixed with a triple spike with known concentrations of $^{229}$Th, $^{233}$U, and $^{236}$U, calibrated against a Harwell Uraninite solution (HU-1) assumed to be at secular equilibrium (Frank et al., 2004). After Fe-coprecipitation, the U and Th fractions were separated and purified on 600 µl columns packed with U-TEVA and prefilter resins in nitric media. The U and Th isotopes ratios were determined using a Multi-Collector inductively coupled plasma mass spectrometer (MC-ICP-MS) Thermo Scientific$^{TM}$ Neptune$^{Plus}$ fitted with a desolvating introduction system (aridus II) following the procedure described by Pons-Branchu et al. (2014). The $^{230}$Th/U ages were calculated from measured atomic ratios through iterative age estimation (Ludwig & Titterington, 1994), using the $^{230}$Th, $^{234}$U, and $^{238}$U decay constants of Cheng et al. (2013) and Jaffey et al. (1971).

#### 3.2.2. Li/Mg Temperature

The Li/Mg ratio was measured on mechanically cleaned samples (20–30 mg each), which were subsequently dissolved in supra-pure 3 N $HNO_3$. Sample solutions were diluted at Ca-100 ppm with a 0.5 N $HNO_3$ ultrapure solution as well as standards before being analyzed using a quadrupole ICP-MS X*series*$^{II}$ (Thermo Fisher Scientific) at the LSCE and following the procedure previously described by Montero-Serrano et al. (2013) and Montagna et al. (2014). Accuracy of Li/Mg results was verified by using external carbonate standards JCp-1 coral, JCt-1 clam, aragonite AK, calcite BAM 3, and the standard JCp-1 was run every five samples in order to correct instrumental drift of a few percentages during the analytical sequence. Finally, the statistic of acquisition being focused on Li and Mg isotopes, analytical uncertainties were ameliorated giving a mean Li/Mg ratio for JCp-1 of 1.494 ± 0.011 mmol/mol (2$\sigma$, n = 18) corresponding to an external reproducibility of 0.74% for Li/Mg ratios. This Li/Mg ratio closely matches the mean Jcp-1 value (1.47 ± 0.05 mmol/mol) obtained from the interlab study published by Hathorne et al. (2013). Li/Mg molar ratios were converted to water temperatures using the exponential regression reported in Montagna et al. (2014) [Li/Mg (mmol/mol) = 5.41 exp(−0.049*T)]. Even though the analytical uncertainty is small, the systematical error of ±0.9°C (2$\sigma$) has been retained for each T°C calculated from this general multispecies calibration (Montagna et al., 2014).

#### 3.2.3. Radiocarbon Dating

Fourteen radiocarbon accelerator mass spectrometry (AMS) dating were performed on planktonic foraminifera *Globigerina bulloides* sampled in the sediment matrix surrounding the CWC fragments in Corals2012-39PC (n = 9) and MD01–2454G (n = 5). About 10 mg, corresponding to about 500 specimens, of *G. bulloides* were sampled from the 250 to 1,000 $\mu$m fraction of the sediment. All samples of foraminifera have been leached with $HNO_3$ at $10^{-2}$ M for 15 min, ultrasonically cleaned for 1 min, and rinsed with MilliQ water to remove superficial contamination (Tisnérat-Laborde et al., 2001). $^{14}$C dating of the *G. bulloides* samples from core Corals2012-39PC was carried out at the Poznan laboratory and the $^{14}$C dates for the core MD01–2454G samples were performed at Beta Analytic Inc., Miami, USA. After subtracting 400 year to account for the average surface ocean reservoir effect, the conventional $^{14}$C ages were calibrated by using the Marine13 calibration data set and the CALIB 7.04 program (Reimer et al., 2013).

## 4. Results

### 4.1. U/Th Dating of CWC and Radiocarbon AMS Dating of Foraminifera

Results of U-series dating of the coral fragments are reported in Table 2. The U concentration of CWC species *L. pertusa* and *M. oculata* displayed a narrow range from 3.09 and 4.85 $\mu$g g$^{-1}$. The initial $\delta^{234}U_i$ values ranged between 144.3‰ and 152.2‰. If the uncertainty of the $\delta^{234}U_i$ is taken into account (Table 2), most of the values fulfill the so-called "strict" ±5‰ to modern sea water value (146.8 ± 0.1‰; Andersen et al., 2010) attesting of a good state of preservation for the CWC samples investigated in this study and implying that the U/Th ages can be considered reliable. Measured $^{232}$Th concentrations are systematically less than 10 ng g$^{-1}$ except for the CWC sampled immediately above the hard-ground at the base of the core Corals2012-39PC (384.5 cm depth), which was found to be much older (~182 ka) than the rest of the CWC (0–11 ka). The U-Th ages of the corals collected from cores Corals2012-39PC and Corals2013-18PC range from 0.25 ± 0.01 to 10.75 ± 0.05 ka BP and from 1.29 ± 0.03 to 8.65 ± 0.09 ka BP (Table 2 and Figure 2). They reveal a continuous but irregular CWC growth pattern throughout the Holocene, in agreement with the results obtained by Lutringer (2003) and Frank et al. (2009) on core MD01–2454G, also located in the SE Rockall margin at a similar water depth (55°31′N–15°39′W, 747 m, Figure 1) (Table 1 and Figure 2).

**Table 2**
*U-Series Ages Obtained for Cold-Water Coral Samples Collected From Sediments of Cores Corals2012-39PC and Corals2013-18PC*

| Depth in core (cm) | Corals species | $[^{238}U]$ (ppm) | | $[^{232}Th]$ (ppb) | | $\delta^{234}U_m$ (‰) | | $^{230}Th/^{238}U$ | | $^{230}Th/^{232}Th$ | | $\delta^{234}U(0)$ (‰) | | Age Cal (ka BP) | | Li/Mg (mmol/mol) | T°C (Li/Mg) |
|---|---|---|---|---|---|---|---|---|---|---|---|---|---|---|---|---|---|
| Coral2012-39PC | | | | | | | | | | | | | | | | | |
| 0.5 | *L. pertusa* | 3.73 | ±0.024 | 0.305 | ±0.0016 | 145.23 | ±1.10 | 0.00356 | ±0.00004 | 138 | ±1.7 | 145.36 | ±1.10 | 0.251 | ±0.014 | 3.77 | 7.36 |
| 1.5 | *M. oculata* | 4.85 | ±0.025 | 0.072 | ±0.0003 | 145.78 | ±1.41 | 0.00361 | ±0.00004 | 772 | ±8.4 | 145.92 | ±1.41 | 0.276 | ±0.006 | 3.75 | 7.49 |
| 4.5 | *M. oculata* | 4.19 | ±0.009 | 2.513 | ±0.0076 | 146.69 | ±0.71 | 0.00749 | ±0.00008 | 40 | ±0.4 | 146.91 | ±0.71 | 0.473 | ±0.079 | | |
| 9.5 | *L. pertusa* | 3.34 | ±0.007 | 8.367 | ±0.0356 | 147.32 | ±1.05 | 0.01532 | ±0.00025 | 20 | ±0.3 | 147.62 | ±1.07 | 0.663 | ±0.320 | | |
| 10.5 | *M. oculata* | 4.60 | ±0.014 | 1.159 | ±0.0010 | 146.93 | ±0.86 | 0.00785 | ±0.00004 | 95 | ±0.5 | 147.21 | ±0.87 | 0.606 | ±0.036 | 3.73 | 7.56 |
| 15.5 | *M. oculata* | 3.94 | ±0.017 | 0.084 | ±0.0004 | 149.03 | ±1.62 | 0.00849 | ±0.00007 | 1255 | ±10.4 | 149.37 | ±1.63 | 0.740 | ±0.011 | 3.76 | 7.44 |
| 17.5 | *L. pertusa* | 3.81 | ±0.019 | 0.065 | ±0.0003 | 151.81 | ±0.98 | 0.00829 | ±0.00006 | 1529 | ±11.9 | 152.15 | ±0.98 | 0.719 | ±0.009 | 3.65 | 8.03 |
| 26.5 | *L. pertusa* | 4.66 | ±0.034 | 0.132 | ±0.0005 | 150.69 | ±1.17 | 0.00973 | ±0.00004 | 1089 | ±4.0 | 151.08 | ±1.17 | 0.854 | ±0.008 | 3.72 | 7.63 |
| 38.5 | *L. pertusa* | 3.59 | ±0.009 | 0.190 | ±0.0002 | 145.98 | ±1.18 | 0.01150 | ±0.00004 | 663 | ±2.3 | 146.43 | ±1.18 | 1.020 | ±0.012 | 3.78 | 7.30 |
| 49.5 | *L. pertusa* | 3.71 | ±0.007 | 7.694 | ±0.0161 | 146.14 | ±1.01 | 0.02242 | ±0.00024 | 34 | ±0.4 | 146.78 | ±1.02 | 1.475 | ±0.271 | | |
| 51.5 | *L. pertusa* | 3.32 | ±0.008 | 0.233 | ±0.0001 | 143.72 | ±1.01 | 0.01595 | ±0.00004 | 696 | ±1.9 | 144.35 | ±1.01 | 1.447 | ±0.014 | 3.60 | 8.31 |
| 58.5 | *L. pertusa* | 3.77 | ±0.006 | 0.234 | ±0.0001 | 146.78 | ±0.90 | 0.01580 | ±0.00005 | 778 | ±2.2 | 147.41 | ±0.90 | 1.431 | ±0.014 | 3.65 | 8.03 |
| 64.5 | *M. oculata* | 4.04 | ±0.009 | 0.384 | ±0.0002 | 147.98 | ±0.82 | 0.01588 | ±0.00004 | 511 | ±1.3 | 148.62 | ±0.83 | 1.427 | ±0.017 | 3.82 | 7.12 |
| 73.5 | *M. oculata* | 4.22 | ±0.014 | 0.300 | ±0.0002 | 147.92 | ±0.95 | 0.02023 | ±0.00007 | 870 | ±2.8 | 148.73 | ±0.95 | 1.854 | ±0.017 | 3.74 | 7.55 |
| 87.5 | *L. pertusa* | 3.71 | ±0.007 | 0.246 | ±0.0002 | 146.43 | ±1.00 | 0.02177 | ±0.00005 | 1005 | ±2.4 | 147.30 | ±1.01 | 2.008 | ±0.015 | 3.64 | 8.11 |
| 98.5 | *M. oculata* | 3.81 | ±0.011 | 0.064 | ±0.0001 | 146.24 | ±0.81 | 0.02373 | ±0.00007 | 4354 | ±12.7 | 147.19 | ±0.82 | 2.214 | ±0.010 | 3.60 | 8.31 |
| 99.5 | *M. oculata* | 3.26 | ±0.005 | 0.217 | ±0.0007 | 148.03 | ±0.78 | 0.02552 | ±0.00019 | 1227 | ±9.3 | 149.05 | ±0.78 | 2.370 | ±0.029 | 3.67 | 7.90 |
| 105.5 | *M. oculata* | 3.81 | ±0.007 | 0.087 | ±0.0001 | 146.89 | ±0.98 | 0.02473 | ±0.00005 | 3321 | ±7.0 | 147.88 | ±0.99 | 2.308 | ±0.010 | 3.70 | 7.78 |
| 109.5 | *M. oculata* | 4.18 | ±0.014 | 0.208 | ±0.0002 | 147.28 | ±1.16 | 0.02710 | ±0.00006 | 1663 | ±4.0 | 148.36 | ±1.16 | 2.530 | ±0.015 | 3.76 | 7.43 |
| 120.5 | *M. oculata* | 4.28 | ±0.006 | 0.109 | ±0.0001 | 147.10 | ±0.55 | 0.02965 | ±0.00011 | 3429 | ±13.4 | 148.29 | ±0.56 | 2.786 | ±0.016 | 3.74 | 7.55 |
| 137.5 | *L. pertusa* | 3.56 | ±0.013 | 0.146 | ±0.0001 | 145.57 | ±0.87 | 0.03870 | ±0.00009 | 2876 | ±6.7 | 147.11 | ±0.88 | 3.673 | ±0.017 | 3.61 | 8.28 |
| 142.5 | *M. oculata* | 4.34 | ±0.003 | 0.154 | ±0.0001 | 145.47 | ±0.93 | 0.03775 | ±0.00007 | 3230 | ±6.1 | 146.98 | ±0.94 | 3.581 | ±0.015 | 3.68 | 7.84 |
| 149.5 | *L. pertusa* | 4.72 | ±0.008 | 1.744 | ±0.0083 | 144.94 | ±0.83 | 0.04066 | ±0.00023 | 352 | ±2.0 | 146.52 | ±0.83 | 3.771 | ±0.069 | | |
| 151.5 | *L. pertusa* | 4.12 | ±0.011 | 0.117 | ±0.0001 | 147.95 | ±0.87 | 0.04000 | ±0.00007 | 4278 | ±7.6 | 149.57 | ±0.88 | 3.797 | ±0.014 | 3.51 | 8.84 |
| 169.5 | *M. oculata* | 4.42 | ±0.010 | 0.204 | ±0.0001 | 145.83 | ±1.25 | 0.04644 | ±0.00012 | 3025 | ±7.8 | 147.70 | ±1.27 | 4.436 | ±0.023 | 3.75 | 7.51 |
| 174.5 | *L. pertusa* | 4.10 | ±0.010 | 0.133 | ±0.0002 | 148.44 | ±1.34 | 0.04743 | ±0.00012 | 4440 | ±11.2 | 150.38 | ±1.36 | 4.527 | ±0.021 | 3.55 | 8.60 |
| 176.5 | *M. oculata* | 4.21 | ±0.007 | 0.087 | ±0.0001 | 146.09 | ±1.08 | 0.05089 | ±0.00013 | 7405 | ±18.5 | 148.15 | ±1.09 | 4.884 | ±0.020 | 3.66 | 7.97 |
| 198.5 | *L. pertusa* | 4.19 | ±0.012 | 0.692 | ±0.0005 | 147.51 | ±0.98 | 0.05688 | ±0.00013 | 1044 | ±2.4 | 149.82 | ±0.99 | 5.430 | ±0.039 | 3.71 | 7.69 |
| 199.5 | *M. oculata* | 3.65 | ±0.008 | 6.192 | ±0.0232 | 143.90 | ±0.74 | 0.05691 | ±0.00023 | 107 | ±0.4 | 145.97 | ±0.75 | 4.998 | ±0.228 | | |
| 209.5 | *M. oculata* | 4.57 | ±0.004 | 0.253 | ±0.0002 | 144.64 | ±0.71 | 0.05467 | ±0.00008 | 3012 | ±4.5 | 146.84 | ±0.72 | 5.258 | ±0.019 | | |
| 217.5 | *M. oculata* | 4.09 | ±0.011 | 0.081 | ±0.0001 | 147.10 | ±1.11 | 0.06233 | ±0.00015 | 9516 | ±23.8 | 149.65 | ±1.13 | 6.023 | ±0.024 | 3.61 | 8.27 |
| 227.5 | *L. pertusa* | 4.45 | ±0.015 | 0.224 | ±0.0003 | 147.56 | ±2.22 | 0.06331 | ±0.00019 | 3793 | ±11.4 | 150.16 | ±2.25 | 6.110 | ±0.038 | 3.63 | 8.12 |
| 235.5 | *L. pertusa* | 4.06 | ±0.008 | 0.146 | ±0.0002 | 149.05 | ±0.67 | 0.06351 | ±0.00014 | 5356 | ±11.9 | 151.68 | ±0.68 | 6.126 | ±0.022 | 3.84 | 7.00 |
| 241.5 | *L. pertusa* | 4.29 | ±0.011 | 0.145 | ±0.0003 | 145.94 | ±0.69 | 0.06292 | ±0.00009 | 5659 | ±7.9 | 148.50 | ±0.70 | 6.085 | ±0.017 | 3.76 | 7.41 |
| 251.5 | *M. oculata* | 4.44 | ±0.015 | 0.096 | ±0.0002 | 147.31 | ±0.88 | 0.06877 | ±0.00016 | 9740 | ±22.5 | 150.14 | ±0.90 | 6.670 | ±0.025 | 3.67 | 7.90 |
| 261.5 | *M. oculata* | 4.37 | ±0.007 | 0.348 | ±0.0003 | 146.71 | ±1.58 | 0.07489 | ±0.00012 | 2863 | ±4.7 | 149.79 | ±1.62 | 7.276 | ±0.033 | 3.74 | 7.53 |
| 265.5 | *M. oculata* | 3.90 | ±0.010 | 0.350 | ±0.0005 | 143.83 | ±1.21 | 0.07754 | ±0.00017 | 2633 | ±5.9 | 146.97 | ±1.24 | 7.562 | ±0.037 | 3.71 | 7.68 |
| 282.5 | *M. oculata* | 4.63 | ±0.009 | 0.114 | ±0.0002 | 143.78 | ±1.20 | 0.08823 | ±0.00016 | 10913 | ±20.0 | 147.38 | ±1.23 | 8.680 | ±0.029 | 3.78 | 7.30 |
| 297.5 | *M. oculata* | 4.08 | ±0.010 | 0.161 | ±0.0004 | 143.70 | ±0.93 | 0.09276 | ±0.00017 | 7166 | ±13.1 | 147.49 | ±0.96 | 9.144 | ±0.031 | 3.79 | 7.26 |
| 307.5 | *L. pertusa* | 4.61 | ±0.007 | 1.231 | ±0.0009 | 146.57 | ±0.89 | 0.09635 | ±0.00016 | 1095 | ±1.8 | 150.55 | ±0.92 | 9.421 | ±0.057 | | |
| 332.5 | *M. oculata* | 4.32 | ±0.009 | 0.963 | ±0.0010 | 143.63 | ±0.68 | 0.10229 | ±0.00019 | 1403 | ±2.6 | 147.81 | ±0.70 | 10.079 | ±0.053 | 3.74 | 7.52 |
| 349.5 | *L. pertusa* | 3.98 | ±0.011 | 9.011 | ±0.0230 | 141.73 | ±1.05 | 0.10735 | ±0.00044 | 151 | ±0.6 | 145.83 | ±1.08 | 10.024 | ±0.324 | | |
| 354.5 | *M. oculata* | 4.57 | ±0.004 | 0.123 | ±0.0001 | 142.42 | ±0.83 | 0.10185 | ±0.00017 | 11564 | ±19.6 | 146.58 | ±0.86 | 10.105 | ±0.029 | 3.79 | 7.28 |
| 359.5 | *M. oculata* | 4.65 | ±0.008 | 0.804 | ±0.0005 | 142.66 | ±0.67 | 0.10847 | ±0.00018 | 1922 | ±3.1 | 147.09 | ±0.69 | 10.752 | ±0.047 | | |
| 384.5 | *L. pertusa* | 4.22 | ±0.007 | 14.453 | ±0.0650 | 87.64 | ±0.82 | 0.90104 | ±0.00351 | 843 | ±3.3 | 146.85 | ±1.74 | 182.576 | ±2.593 | | |
| Corals2013-18PC | | | | | | | | | | | | | | | | | |
| 27.5 | *L. pertusa* | 3.42 | ±0.005 | 0.765 | ±0.0007 | 147.45 | ±0.73 | 0.01490 | ±0.00005 | 204 | ±0.7 | 148.05 | ±0.73 | 1.293 | ±0.033 | | |
| 92.5 | *L. pertusa* | 3.33 | ±0.004 | 0.191 | ±0.0002 | 145.26 | ±0.75 | 0.03895 | ±0.00008 | 2084 | ±4.4 | 146.82 | ±0.76 | 3.694 | ±0.017 | 3.94 | 6.5 |
| 146.5 | *L. pertusa* | 3.09 | ±0.003 | 0.215 | ±0.0002 | 147.50 | ±0.82 | 0.05456 | ±0.00009 | 2207 | ±4.2 | 149.74 | ±0.83 | 5.227 | ±0.023 | 3.69 | 7.8 |
| 178.0 | *L. pertusa* | 3.11 | ±0.012 | 0.255 | ±0.0007 | 151.82 | ±3.01 | 0.05690 | ±0.00031 | 2098 | ±11.6 | 154.20 | ±3.06 | 5.436 | ±0.056 | 3.93 | 6.5 |
| 247.5 | *L. pertusa* | 3.81 | ±0.009 | 0.255 | ±0.0003 | 146.97 | ±1.40 | 0.06292 | ±0.00010 | 2855 | ±4.5 | 149.54 | ±1.42 | 6.069 | ±0.026 | 3.71 | 7.7 |
| 288.5 | *L. pertusa* | 3.27 | ±0.003 | 1.583 | ±0.0011 | 144.99 | ±0.76 | 0.06866 | ±0.00012 | 431 | ±0.8 | 147.72 | ±0.78 | 6.528 | ±0.078 | 3.76 | 7.4 |
| 339.0 | *L. pertusa* | 4.15 | ±0.006 | 0.483 | ±0.0004 | 140.35 | ±0.98 | 0.07360 | ±0.00017 | 1935 | ±4.5 | 143.27 | ±1.00 | 7.175 | ±0.038 | 3.63 | 8.1 |
| 359.0 | *L. pertusa* | 3.84 | ±0.005 | 0.326 | ±0.0003 | 144.53 | ±1.19 | 0.07790 | ±0.00017 | 2787 | ±6.0 | 147.69 | ±1.21 | 7.595 | ±0.036 | 3.68 | 7.9 |
| 392.0 | *L. pertusa* | 3.21 | ±0.037 | 0.104 | ±0.0007 | 142.84 | ±2.21 | 0.08789 | ±0.00064 | 8254 | ±60.8 | 146.40 | ±2.27 | 8.650 | ±0.089 | 3.84 | 7.0 |
| *M2000-25BX* | | | | | | | | | | | | | | | | | |
| Top | *L. pertusa* | | | | | | | | | | | | | Living | Coral | 3.60 | 8.3 |

*Note.* Li/Mg ratios measured in CWC aragonite for corals studied here and deduced temperatures are also displayed with uncertainties of about 0.73% for Li/Mg ratios and ±0.9°C for each reconstructed seawater temperature (Montagna et al., 2014).

**Table 3**
*Calibrated AMS $^{14}C$ Age Determined on Planktonic Foraminifera Sampled in Corals2012-39PC and MD01–2454G (Data Taken From* Lutringer, 2003*)*

| Core | Depth interval (cm) | | Uncorrected C14 age yrs | Calendar age BP yrs | 1$\sigma$ age range yrs |
|---|---|---|---|---|---|
| Corals2012-39PC | 4–5 | *G. bulloides* | 1,385 ± 30 | 932 | 899–962 |
| Corals2012-39PC | 49–50 | *G. bulloides* | 2,690 ± 50 | 2,395 | 2,320–2,453 |
| Corals2012-39PC | 99–100 | *G. bulloides* | 5,115 ± 35 | 5,489 | 5,447–5,543 |
| Corals2012-39PC | 149–150 | *G. bulloides* | 5,380 ± 35 | 5,750 | 5,696–5,820 |
| Corals2012-39PC | 199–200 | *G. bulloides* | 6,880 ± 90 | 7,390 | 7,305–7,471 |
| Corals2012-39PC | 249–250 | *G. bulloides* | 7,900 ± 50 | 8,363 | 8,315–8,407 |
| Corals2012-39PC | 299–300 | *G. bulloides* | 9,200 ± 50 | 10,008 | 9,926–10,109 |
| Corals2012-39PC | 349–350 | *G. bulloides* | 10,010 ± 50 | 11,006 | 10,926–11,104 |
| Corals2012-39PC | 384–385 | *G. bulloides* | 11,200 ± 60 | 12,689 | 12,626–12,741 |
| MD01–2454G | 30 | *G. bulloides* | 2,940 ± 40 | 2,725 | 2,680–2,770 |
| MD01–2454G | 60 | *G. bulloides* | 4,030 ± 40 | 4,035 | 3,920–4,150 |
| MD01–2454G | 89 | *G. bulloides* | 4,950 ± 40 | 5,310 | 5,230–5,390 |
| MD01–2454G | 150 | *G. bulloides* | 5,220 ± 40 | 5,575 | 5,510–5,640 |
| MD01–2454G | 214 | *G. bulloides* | 7,280 ± 40 | 7,735 | 7,660–7,810 |

*Note.* $^{14}C$ ages were converted into calendar years (cal. yr BP, BP = AD 1950) by using the Marine13 calibration data set and the CALIB 7.04 program (Reimer et al., 2013). A mean reservoir effect of ~400 years has been used.

$^{14}C$ ages obtained on planktonic foraminifera in cores MD01–2454G (Lutringer, 2003) and Corals2012-39PC are also reported in Table 3 and potted in Figure 2 for comparison with vertical corals accumulation (U-Th ages). The relationships between depth and $^{14}C$ ages obtained on planktonic foraminifera are similar for cores MD01–2454G and Corals2012-39PC. For a given depth, CWC U-Th ages are younger than foraminifera $^{14}C$ ages over both entire cores. This age offset reaches a maximum (2 ka for core MD01–2454G and 3 ka for core Corals2012-39PC) around 100 cm in both cores and tends to decrease toward the top and the bottom of the cores. The timing of the increase of this offset during the Holocene is difficult to be precisely determine due to the low number of C-14 dating available but seems to occur at the Mid-Holocene (around 5.5 ka for core MD01–2454G and around 7–6 ka for core Corals2012-39PC). The late-Holocene is characterized by an apparent sudden increase in sediment accumulation, reaching ~110 cm ka$^{-1}$ in both cores at depth interval from 150 to 90 cm (corresponding to radiocarbon dating of planktonic foraminifera centered around 5.5 ka BP).

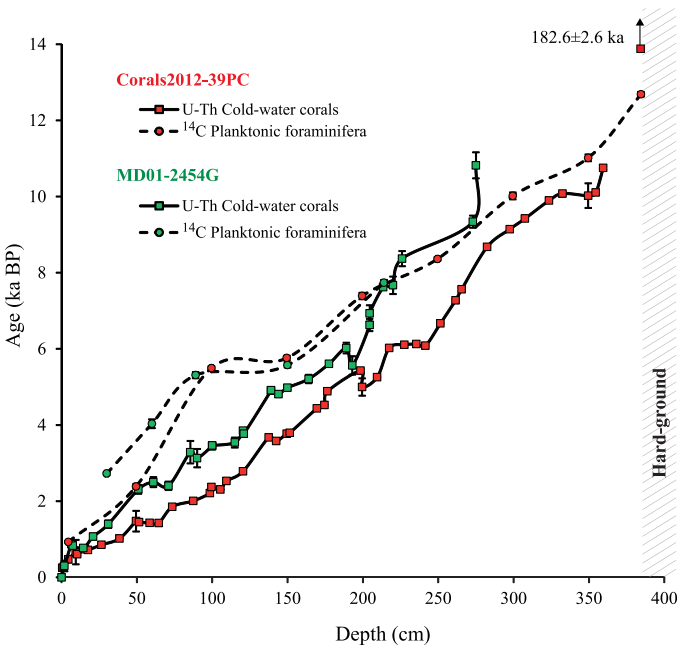


**Figure 2.** Age-depth profile of cores Corals2012-39PC (red) and MD01–2454G (green). U-Th ages (solid line) were measured on CWC collected in cores Corals2012-39PC (this study) and MD01–2454G (Frank et al., 2009). $^{14}C$ AMS ages (dashed line) were measured on planktic foraminifera *G. bulloides* on both cores (this study).

### 4.2. Li/Mg and Holocene Bottom Water Temperatures

Before extrapolating the temperature from the Li/Mg ratio value, as reported by Montagna et al. (2014), we first verified this exponential regression by comparing the Li/Mg temperature measured in a living coral from the SW Rockall Trough (sample Rockall-2000) collected in 2,000 at 773 m water depth and the measured temperature of the deep-water environments. The living coral indicated a Li/Mg value of 3.60 ± 0.12 mmol/mol which translates into a temperature of 8.3 ± 0.9°C. This temperature estimate is similar to the modern seawater temperature measured by CTD at this depth (8.1°C, Dubois-Dauphin, 2017; 8.3°C; Mienis et al., 2007). However, due to internal waves, the temperature can vary daily by 2°C (e.g., between 6.7 and 8.8°C in a day at 800 m; Duineveld et al., 2007; Mienis et al., 2007). Therefore, the CWC seem to record a temperature averaged over the lifetime of the coral polyp and thus fully integrate the tidal variability.

The fossil CWC of cores Coral2012-39PC and Corals2013-18PC displayed a narrow range of Li/Mg ratios from 3.51 ± 0.06 to 3.94 ± 0.07

mmol mol$^{-1}$. The temperature obtained using the Li/Mg ratios ranged from 7.0 ± 0.9 to 8.8 ± 0.9°C in core Coral2012-39PC (n = 35) and from 6.5 ± 0.9°C to 8.1 ± 0.9 in core Corals2013-18PC (n = 8). No notable temperature gap linked to CWC genera was observed in this case. In core Coral2012-39PC, the early Holocene (before 6 ka) is associated with slightly lower Li/Mg temperature (7.0 ± 0.9°C to 7.9 ± 0.9°C) than the late-Holocene (7.4 ± 0.9 to 8.8 ± 0.9°C) (Figure 3b). Li/Mg temperatures vary from 7°C to 9°C with minor increases of around 1°C observed at 6, 4.5, 3.7, 2.2 ka and, to a lesser extent, at 1.4 ka. Two CWC fragments collected in the deepest core, Corals2013-18PC (790 m), indicated a cold temperature (6.5 ± 0.9°C) at 5.4 and 3.9 ka (Figure 3b). This is ∼1.5°C below the temperature recorded for the same period in core Coral2012-39PC, which was located 50 m shallower.

## 5. Discussion

### 5.1. Climatic Control of Growth Rates and Abundance of CWC in the SW Rockall Trough

The U-Th ages of the corals samples from cores Corals2012-39PC and Corals2013-18PC cover the Holocene (0.25 ± 0.01 to 10.75 ± 0.045 ka BP) with an older CWC samples (∼182 ka BP) collected immediately above the hard-ground at the base of the core Corals201239PC (384.5 cm depth) (Figure 2). This suggests that Holocene CWC developed on an ancient reef, which was active during Marine Isotope Stages (MIS) 7.1. Furthermore, it confirms that coral mounds in the Rockall Trough were inactive during glacial times and that the CWC corals preferentially reestablished on the hard substrates formed by ancient reefs slightly after the Younger Dryas cold events (12.9–11.5 ka BP). This finding is in agreement with the previously proposed long-term cycle of CWC mound growth (Frank et al., 2009; Mienis et al, 2006; Pirlet et al., 2011).

The vertical CWC accumulation rates in core Corals2012-39PC, estimated from the relationship between the U-Th age of CWC and its depth within the core (Figure 2), displayed a range from <15 to >150 cm ky$^{-1}$ (mean values of 33 cm ka$^{-1}$). This is significantly higher than accumulation rates observed in core MD01–2454G (mean values of 25 cm ka$^{-1}$, Figure 2). Certain similarities can be observed between the evolution of the CWC accumulation rates obtained for core Corals2012-39PC and for core MD01–2454G (Figure 2): low accumulation rates (16.0 and 15.7 cm ka$^{-1}$, respectively) are observed for the interval 6.5–8.6 ka whereas high accumulation rates (47 and 40 cm ka$^{-1}$, respectively) are observed for the late-Holocene (0–6 ka) and, to a lesser extent, for the period between 10 and 8.5 ka. In detail, the CWC accumulation rates displayed a "stepped" shape with "plateaus" indicating elevated (high) CWC accumulation rates (i.e., core depth intervals characterized by CWC having the same or very similar U-Th age). Interestingly, several of these "plateaus" occur at similar time intervals in both cores, even though they were collected from different mound structures (Figure 2).

Our 53 U-Th dated CWC, together with published data from various CWC mounds in the SW Rockall Trough (Figure 1 and Table 1), form a composite record of 118 U-Th dated CWC covering the Holocene (11–0 ka). In order to highlight the overall age distribution characteristics, the data were processed to produce a probability density plot (see captions for details) which is shown in Figure 3 together with the cumulative number of ages and a histogram of the number of ages binned at 200 year intervals. In this context, pronounced age clusters indicate periods of sustained coral proliferation when suitable environmental conditions prevailed, whereas pronounced gaps or decreases in the coral age record are interpreted as reflecting periods of limited coral growth.

Results have shown that the early Holocene (10–6 ka) is marked by a low abundance of CWC in comparison to the rest of the Holocene. CWC abundance is higher in the late-Holocene (6–0 ka) but is variable. In detail, time intervals 0–0.3, 0.6–0.8, 1.2–1.8, 2.2–2.5, 3.4–3.8, 4.8–5, 5.2–5.6, and 6–6.2 ka are characterized by a high occurrence of CWC, with up to eight dated CWC per 200 years (Figure 3). Conversely, very low incidences of CWC are found at time intervals 0.9–1.2, 1.5–2.1, 2.6–3.4, 3.9–4.8 ka, and to a lesser extent around 0.3–0.6 ka. Time intervals of low CWC proliferation fit well with those identified by Frank et al. (2009) at 1.8–2.0 ka, 4.2–4.8 ka but the hiatus they reported between 6 and 8.2 ka has been partially filled in with our new data. This indicates strong regional millennial variability in the CWC proliferation on coral mounds of the SW Rockall margin.

The mid-Holocene proliferation of CWC observed at 5.5 ka BP coincides with a general decrease of ice-rafted debris (IRD) deposits (Figures 3d and 3e) which were derived from core VM29–191 located at the SW Rockall Trough by Bond et al. (1997, 2001) (Figure 1). There is also an apparent correlation between the

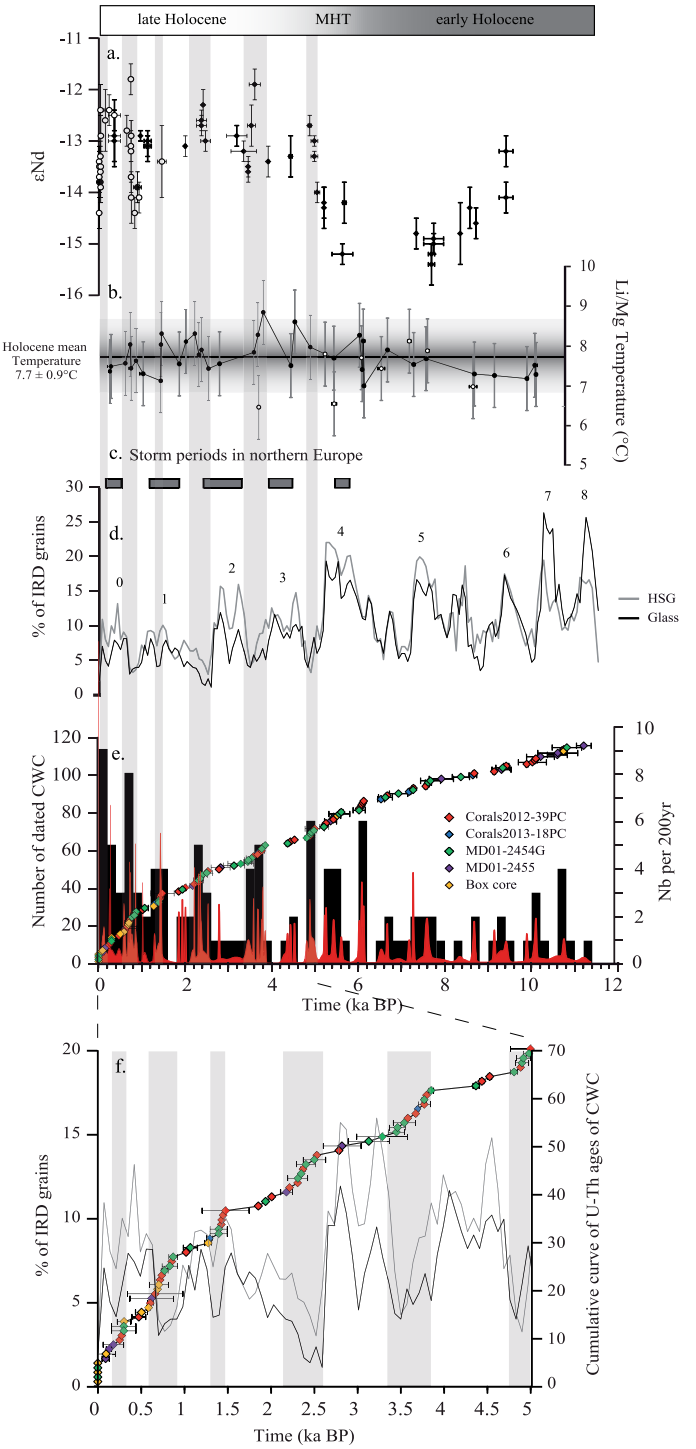


**Figure 3.** Compilation of U-Th dates (see Table 1 for references), Li/Mg temperature (b) and εNd values (a, Colin et al., 2010; Copard et al., 2012) obtained from CWC collected on the SW Rockall Bank (see Figure 1). Note that Li/Mg temperature and εNd are not available for all dated CWC. They are compared with (d) IRD (Glass and Hematite Stained Grains—HSG) abundance in core VM29–191 (Bond et al., 1997) and (c) storm periods in Northern Europe (Sorrel et al., 2012). In plot e, cumulative curve of U-Th dates obtained on individual CWC (dots) is reported with their error bar. In order to take into account the uncertainty of each data point and their overlapping, the probability density plot (red curve, unitless) was calculated using the Isoplot 4 add-in program for Microsoft *Excel*. The number of CWC ages per 200 years (black bars) are reported. The plot f is a zoom of the last 5 ka BP of the cumulative curve of U-Th dates obtained on individual CWC (dots) and the IRD (Glass and Hematite Stained Grains—HSG) abundance in core VM29–191 (Bond et al., 1997).

millennial cycles of enhanced/reduced CWC abundance and the IRD records (Figures 3d and 3e). This relationship is especially striking for the late-Holocene (0–5 ka) where time intervals of reduced CWC proliferation at 0.3–0.6, 0.9–1.2, 1.5–2.1, 2.6–3.4, and 3.9–4.8 ka are coeval with cold phases and increased drift-ice events (high IRD) while intervals of increased CWC occurrence are associated with warm phases and decreases in North Atlantic drift-ice (low IRD). Such results imply a climatic control on the CWC growth of the coral mounds in the SW Rockall Trough located at about 750 m water depth.

### 5.2. Potential Environmental Conditions Responsible for Spatial Distribution of CWC in the SW Rockall Trough

At the present time, it has been demonstrated that strong slope currents (internal waves and baroclinic tidal currents), which are amplified by the high density gradient at thermocline depth, are likely to promote CWC proliferation (Mohn et al., 2014; White & Dorschel, 2010). On SE edge of the Rockall Bank, it has been demonstrated that diurnal tidal waves trapped by the topography of coral mounds induce local currents, which are amplified more than five times as compared to the surroundings (Duineveld et al., 2007; Mienis et al., 2007; van Haren et al., 2014; White & Dorschel, 2003). These internal tidal waves induce a strong semidiurnal vertical movement (excursion of 250–400 m) of cold and warm water along the slope of the SW Rockall Trough (Van Haren et al., 2014). The daily temperatures can increase as much as 2°C at 810 m water depth and decrease rapidly upward and downward in the water column by around 1°C at 1,000 and at 630 m (Mienis et al., 2007, 2009; van Haren et al., 2014). Therefore, the high tidal waves and excursion length are thought to influence the depth of CWC mound occurrence, which seems to be limited to ~600 m (Duineveld et al., 2007; Mienis et al., 2006; van Haren et al., 2014; White & Dorschel, 2010).

In addition to preventing living corals from being buried, strong currents around the mounds play an important role in providing food particles to the CWC by downslope advection of surface productivity (Mohn et al., 2014; White & Dorschel, 2010) or by resuspension of particles from the bottom resulting in nepheloid layers (Frederiksen et al., 1992). A conceptual model by White et al. (2005), proposed that the main food source for Rockall CWC derives from enhanced primary productivity over the Rockall Bank, due to deep-winter convection that brings nutrient-rich water to the surface in early spring causing a spring bloom (Holliday et al., 2000). The organic matter is retained on the Rockall Bank by the anticyclonic circulation around the bank and is eventually exported downslope by Ekman transport. Finally, the diurnal trapped waves play an important role in maintaining (food) particles in suspension along the slope. This process, which enables a continuous input of fresh organic material to the CWC, was later confirmed by Duineveld et al. (2007) in an integrated study of food web, particle flux, and current dynamics over the Rockall Bank slope. They observed that on a daily time scale the concentration of food particles over the CWC mounds varies with temperature and current direction. Food flux is carried by relatively warm and saline water most likely coming from upslope and flowing in an SSE direction.

Since the thermocline (and the associated residual currents produced by its contact with the slope) has been identified as the main factor explaining the spatial distribution of CWC mounds in the NE Atlantic, its temporal stability is suspected to be the main driver producing favorable conditions for mound growth over long time periods (White & Dorschel, 2010). For instance, it has been suggested that a shallowing of the thermocline together with a high ice-rafted debris (IRD) flux could be responsible for the CWC colony collapse observed during glacial times (Frank et al., 2011; Rüggeberg et al., 2016; White & Dorschel, 2010). Consequently, the observed changes in the distribution of CWC in the SW Rockall Trough at intermediate water depth (between 740 and 790 m) during the Holocene could be attributed to (1) changes in the vertical stratification of the water column (depth and structure of the thermocline) affecting the strength or direction of the slope residual currents, (2) changes in the surface productivity or changes in the processes transmitting food particle flux to the CWC mounds, (3) changes in the detrital inputs during IRD events, or (4) a combination of these processes.

### 5.3. Mid-Holocene Changes in the Abundance of CWC

By definition, the permanent thermocline lies underneath the winter mixing zone, but in the Rockall Trough it also marks the interface between the warm Central Waters and the colder and fresher Labrador Sea Water (LSW) identified at 1,200 m in the Rockall Trough (Ellett & Martin, 1973; Holliday et al., 2000; New & Smythe-Wright, 2001). The favorable environmental window for CWC growth at this interface may have been

sensitive to past circulation changes. The increase in the occurrence of CWC at the SW Rockall Trough margin in the mid-Holocene (6–7 ka) is coeval with major hydrological reorganisation in the NE Atlantic (Colin et al., 2010; Thornalley et al., 2009). In the North Atlantic, εNd can be used to distinguish between water derived from the subpolar region (MNAW, LSW, and SAIW) and water originating from the subtropical Atlantic (NEAW and MSW) (Dubois-Dauphin et al., 2017). Holocene records of seawater εNd obtained on CWC from the SW Rockall Trough (Figure 3) indicate that the mid-Holocene reorganization is marked by a change in the origin of water masses flowing into the study area (Colin et al., 2010; Copard et al., 2012). The extremely low εNd values observed in the early Holocene, when CWC occurrence was low in the SW Rockall Trough, attest of a greater influence of subpolar water, specifically water originating from the Labrador Sea (SAIW; Colin et al., 2010). During the Holocene, changes in wind fields and in the extension of the SPG could have modified the stratification of the water column by affecting the density gradient and the thickness of the convective winter mixing layer (Wade et al., 1997) and may thus have controlled the proliferation of CWC in the Rockall Trough.

Wade et al. (1997) proposed that the SAIW, which is characterized by low salinity and temperature (4–7°C, 34.7–34.9 PSU; Pollard et al., 1996) underneath the Central water, plays an important role in the stability of the NE Atlantic water column. They demonstrated that the presence of relatively "pure" SAIW in the NE Atlantic prevents deep winter mixing due to enhanced stratification. In contrast, in the absence of a well-defined SAIW layer, as in the Rockall Trough from 6 ka onward, the weaker density gradient allows deep winter convection (Ellett et al., 1986; Holliday et al., 2000). Additionally, the LSW did not exist before 7 ka BP due to the freshwater input from the residual Laurentide Ice Sheet which prevented deep convection in the Labrador Sea (Hillaire-Marcel et al., 2001; Hoogakker et al., 2015; Solignac et al., 2004). We have no information about the water mass that occupied the depth range of modern-LSW, but the LSW production in the Labrador Sea was potentially replaced by shallower convection (García-Ibáñez et al., 2015), which eventually enhanced the production of intermediate water. The incursion of SAIW at today's thermocline depth in the early Holocene could have modified the shape or the position of the thermocline. The slightly lower Li/Mg temperature obtained from CWC core Corals2012-39PC (742 m) for the early Holocene compared to the rest of the Holocene may be compatible with a greater proportion of SAIW. Interestingly, this tendency is reversed in the deeper core (Corals2013-18PC, 790 m). The decrease in temperature observed in the mid-Holocene and late-Holocene could be related to the settling of the LSW. The difference in the temperature recorded in the two cores potentially reflects changes in the past structure of the thermocline. Before 7 ka, the 740–790 m depth interval is remarkably homogeneous in terms of temperature, while a gradient (~1°C) is observed thereafter. A low-density gradient at the depth of the CWC would have reduced the local currents and vertical shifts of warm and cold waters and eventually would have led to less favorable conditions for CWC proliferation in the early Holocene. In addition, the presence of a relatively higher proportion of SAIW at intermediate depth would have moved the permanent thermocline to a shallower depth creating a thinner mixed layer and thus decreasing nutrient availability and surface productivity. This would be in agreement with the low primary productivity reconstructed by Bond et al. (1997) in the SW Rockall Trough for the early Holocene.

Between 6 and 5 ka, the progressive installation of a modern-like circulation, with a higher proportion of ENAW at CWC mound depth (Colin at al., 2010) coincides with an increase in the occurrence of CWC as well as an increase of the CWC accumulation rate (Figure 3). It has been previously shown that CWC mound growth is primarily controlled by CWC growth (the trapping framework) but sediment input provides stability to the CWC mound structure and is thus also necessary for mound accumulation (Hebbeln et al., 2016). The sediment matrix surrounding the CWC fragments in both cores MD01–2454G and Corals2012-39PC is marked by an increase of the offset between CWC U-Th ages and foraminifera $^{14}C$ ages at the mid-Holocene which reach a maximum (2–3 ka) around 3.5–2 ka BP (U-Th age obtained on CWC) (Figure 2). According to $^{210}Pb$ measurements, this large offset of ages cannot be explained by the biological activity (bioturbation) which has been estimated to be around 10 cm at the top of the CWC mounds of the SW Rockall Trough margin (de Haas et al., 2009). Consequently, we can hypothesize that this regional offset of ages between the matrix and CWC is probably due to the reworking of older sediments (Lutringer, 2003; Mienis et al., 2009) implying an intensification of bottom current velocity. This is also associated with major hydrological reorganization of the middepth circulation in the SW Rockall Trough marked by an increase contribution of water masses originating from the subtropical North Atlantic (Figure 3a) (Colin et al., 2010).

This increase in bottom current velocity could thus be responsible for the apparent increase in sediment supply and CWC accumulation rates observed in both cores at the mid-Holocene (Figure 2). Therefore, radiocarbon dating obtained on foraminifera collected on marine cores from these CWC mounds cannot be used to establish a chronological time scale for such marine sequences.

### 5.4. Millennial Changes in the Abundance of CWC

After the mid-Holocene transition (from 5.5 to 0 ka) CWC occurrence started to vary according to millennial cycles of enhanced/reduced coral occurrences, which are tuned to the North Atlantic ice-rafted debris (IRD) cycles (Bond et al., 1997, 2001; Figure 3). Time intervals of reduced CWC proliferation, at 0.3–0.6, 0.9–1.2, 1.5–2.1, 2.6–3.4, and 3.9–4.8 ka, are coeval with cold periods associated with higher IRD deposition rates (Figure 3). On the contrary, time intervals of slight increase of Li/Mg temperatures coincide with time intervals of increased CWC abundance (1.2–1.8, 2.2–2.5, 3.4–3.8, 4.8–5, 5.2–5.6, and 6–6.2 ka) (Figure 3b). Consequently, the environmental changes accompanying the Bond cycles probably influenced the local hydrodynamic, food supply, and/or sedimentation input around the mounds and eventually affected CWC proliferation.

An enhanced influx of terrigenous material above the mound during IRD events would have resulted in unusually high detrital input for this region which is located far from continental sources. IRD, which are typically composed of a mixture of clay-sized to sand-sized rock fragments, are observed at the base of the core below the first observed CWC (at ∼11 ka). It has been proposed that IRD input could explain the absence of CWC for the Challenger Mound during the last glacial period (Belgic Mound Province; Pirlet et al., 2011). To a lesser extent during the Holocene, the millennial-scale variations in coarse IRD deposition could have been high enough to temporarily limit the proliferation of CWC. High detrital flux is known to be a limiting factor for CWC proliferation (Roberts et al., 2009) and the bottom currents may not have been efficient in eliminating the coarse particles brought to the coral mounds by drift-ice. However, it has been shown that coral growth rate is an order of magnitude higher than the general sedimentation rate (de Haas et al 2009; Hebbeln et al., 2016) and therefore only very high sedimentation supply may have had a negative influence on CWC growth (Victorero et al., 2016). This suggests that IRD deposition is probably not sufficient to have a direct negative impact on CWC growth. Nevertheless, coarse IRD sediments in combination with vigorous currents may lead to abrasion of the CWC and hence may have a negative influence on coral growth. In addition, it is also possible that coarse IRD deposits facilitate the installation of planula as suggested in previous studies. If IRD deposition is the main factor controlling CWC growth, then this millennial-scale variability in the CWC proliferation should be observed at a regional scale, independently of the water depth.

The IRD events have also been linked to sea surface cooling of the NE Atlantic, and modifications of the hydrology of deep-water masses in the NE Atlantic with a decrease of the intensity of the Iceland Scotland Overflow Water (Bianchi & McCave, 1999). Sorrel et al. (2012) have shown that IRD events are also associated with stormy periods in Northern Europe (Figure 3). Strong winds during these cold events are also reported at higher latitudes, in Greenland and Iceland (O'Brien et al., 1995). The Holocene millennial-scale variations in SST of the NE Atlantic are thought to be tied to changes in the intensity and the extend of the SPG (Miettinen et al., 2012; Thornalley et al., 2009). Moreover, it has been proposed that the variations in the extension of the SPG could be driven by the strength and location of westerly winds (Colin et al., 2010; Copard et al., 2012) and thus be correlated to the storm tracks in the North Atlantic sector (Sorrel et al., 2012). Overall, the past millennium is the best documented period in climate records as well as in our dataset. The cold period known as the Little Ice Age (LIA), centered on ∼400 year BP, notably coincides with a reduced occurrence of CWC, an increase of the North Atlantic IRD (Bond et al., 1997), a westward contraction of the SPG (Copard et al., 2012; Thornalley et al., 2009) associated with a southward displacement of the Westerlies, presumably resembling a dominant negative NAO state condition (Copard et al., 2012; Miettinen et al., 2011, 2012), and high storminess in Northern Europe (Sorrel et al., 2012). In contrast, the warm interval in European history between ∼750 and 1,050 year BP, known as the Medieval Climate Anomaly (MCA), is associated with high CWC occurrence. It has been recently shown by simulation that this westward contraction observed in the SPG between the MCA and the LIA could be triggered by anomalously large freshwater export from the Arctic and can mainly be attributed to internal climate variability (Moreno-Chamarro et al., 2017) instead that a phase shift of the NAO. Nevertheless, older events of decrease of CWC abundance are not systematically associated to changes in the position of the SPG as reconstructed by the εNd values

measured in CWC (Figure 3; Colin et al., 2010) but are coeval to IRD events and periods of higher storminess in northern Europe (Figure 3). Changes in storminess and, more generally, in the wind field could have affected, in many ways, the surface productivity as well as the transport of food particles to the CWC mounds. An increase in storminess is likely to cause an intensification of the mixing that could be at the origin of the enhanced surface productivity reported in the SW Rockall Trough by Bond et al. (1997) during IRD events. On the other hand, changes in wind fields may have impacted upon the cyclonic circulation over the Rockall Bank and the Ekman transport permitting the transportation of food particles downslope to the CWC mounds.

We note that periods of low CWC proliferation, linked to IRD events, are coeval with a slight but systematic decrease in Li/Mg temperatures measured using CWC from Coral2012-39PC (Figure 3). In contrast, a higher proliferation of CWC is associated with a slight increase in Li/Mg temperature. The temperature difference is about 1°C, which is close to the uncertainty of each data point (0.9°C). If confirmed, this temperature difference would indicate that thermocline structure has been affected by the IRD event either by transmission of the surface cooling down to thermocline depth or by a shallowing/contraction of the thermocline. The latter seems to be incompatible with the increase in wind stress and cooling at the surface that, instead, would have resulted in a deeper surface mixed layer. In contrast, fresh water flux from drift-ice melting may have locally caused marked surface layer stratification and a decrease in the mixed layer depth. We can thus hypothesize that IRD events shift the permanent thermocline and associated current regime to a shallower depth permitting the resuspension and transport of sediments and organic matter from the Rockall Bank to the CWC reefs installed along the bank slope. Such a scenario could potentially explain the older (redeposited) sediments observed for the mid-Holocene in the studied cores.

## 6. Conclusions

U-Th ages and Li/Mg temperatures have been obtained for *L. pertusa* and *M. oculata* CWC fragments sampled on two different coral mounds in the SW Rockall Trough. 53 CWC samples were dated and these were compiled with U-Th dates previously published for other CWC mounds located in a restricted area of the SW Rockall Trough margin, between 740 and 790 m water depth. We have established a very detailed record of the abundance of CWC during the Holocene. By comparing our data with other paleo-climate records we have sought to better constrain the environmental conditions controlling CWC proliferation at the SW Rockall Trough margin. Our findings show that during the Holocene, CWC growth was influenced by millennial-scale North Atlantic climate variability.

Long-term changes in the CWC occurrence on coral mounds of the SW Rockall indicate a mid-Holocene increase that is coeval with a major reorganization of the hydrology in the North Atlantic and a decrease in IRD deposition. Before ~7 ka, a greater contribution of SAIW at intermediate water depth and the absence of the LSW at greater water depth are likely to have increased the stratification of the water column. Under such hydrological conditions, the shallowing/shrinking of the thermocline may have reduced the near-bottom currents at mound depth while a thinner surface mixed layer may have limited the primary productivity. The combined processes seem to have caused unfavorable conditions for CWC explaining their low occurrence in the early Holocene.

During the late-Holocene, our record is marked by the emergence of alternating intervals of low/high CWC occurrence which correlate to millennial oscillations in the IRD record. Favorable environmental conditions for CWC growth in the SW Rockall Trough seem to be reached when drift-ice and storminess over the NE Atlantic realm are low. Further investigations will be necessary in order to determine whether the most important controlling factor in these millennial-to-centennial oscillations in CWC abundance was detrital flux (IRD input) or the prevailing hydrological conditions. It would be then important to constrain terrigenous fluxes (IRD), sedimentary sources and sorting of the detrital material in order to further examine the influence of sedimentation and deep-sea processes on CWC growth. The analysis of CWC collected at different depths along the Rockall slope would be particularly interesting for determining whether the CWC migrated to another, more suitable, depth range. Furthermore, Li/Mg temperature measured on CWC located at different depths could provide valuable information regarding thermocline structure and its variability. Further investigation will be also necessary to reconstruct, at very high temporal resolution, surface productivity of the Rockall Trough and to establish its potential impacts on CWC mound growth. Finally, our

results indicate the quasi-permanent presence of CWC in the SW Rockall Trough, which means that CWC constitutes a suitable archive for further investigations of past hydrology of the intermediate water masses in the Rockall Trough.

**Acknowledgments**
We would like to thank the crew and technicians on board the RV Pelagia. The research leading on which this study is based has received funding from the French National Research Agency "Investissement d'Avenir" (ANR-10-LABX-0018), the HAMOC project ANR-13-BS06-0003, and the MISTRALSENVIMED/Boron Isotope and Trace Elements project. Analyses have been done on instruments from the analytical platform PANOPLY. We also thank Arnaud Dapoigny and Louise Bordier for their support with U/Th dating and Li/Mg analyses of cold-water corals. The two anonymous reviewers are also thanked for their constructive comments on the manuscript. Furu Mienis is supported financially by the Innovational Research Incentives Scheme of the Netherlands Organisation for Scientific Research (NWO-VENI/VIDI). All data of this study are reported in tables of this manuscript. This is LSCE contribution 6465.

## References

Andersen, M. B., Stirling, C. H., Zimmermann, B., & Halliday, A. N. (2010). Precise determination of the open ocean $^{234}U/^{238}U$ composition. *Geochemistry, Geophysics, Geosystems*, *11*, Q12003, https://doi.org/10.1029/2010GC003318

Bianchi, G. G., & McCave, I. N. (1999). Holocene periodicity in North Atlantic climate and deep ocean flow south of Iceland. *Nature*, *397*(6719), 515–517.

Bond, G., Kromer, B., Beer, J., Muscheler, R., Evans, M. N., Showers, W., et al. (2001). Persistent solar influence on North Atlantic climate during the Holocene. *Science*, *278*, 1257–1266.

Bond, G., Showers, W., Cheseby, M., Lotti, R., Almasi, P., de Menocal, P., et al. (1997). A pervasive millennial-scale cycle in the North Atlantic Holocene and glacial climates. *Science*, *294*, 2130–2136.

Bower, A. S., Le Cann, B., Rossby, T., Zenk, W., Gould, J., Speer, K., et al. (2002). Directly measured mid-depth circulation in the northeastern North Atlantic Ocean. *Nature*, *419*(6907), 603–607.

Cheng, H., Lawrence Edwards, R., Shen, C.-C., Polyak, V. J., Asmerom, Y., Woodhead, J. D., et al. (2013). Improvements in $^{230}Th$ dating, $^{230}Th$ and $^{234}U$ half-life values, and U-Th isotopic measurements by multi-collector inductively coupled plasma mass spectrometry. *Earth and Planetary Science Letters*, *371–372*, 82–91.

Colin, C., Norbert, N., Copard, K., & Douville, E. (2010). Neodymium isotopic composition of deep-sea corals from NE Atlantic: Implications for past changes of hydrology during the Holocene. *Quaternary Science Reviews*, *29*(19–20), 2509–2517.

Copard, K., Colin, C., Henderson, G. M., Scholten, J., Douville, E., Sicre, M. A., et al. (2012). Late Holocene intermediate water variability in the northeastern Atlantic as recorded by deep-sea corals. *Earth and Planetary Science Letters*, *313–314*, 34–44.

Davies, A. J., Wisshak, M., Orr, J. C., & Roberts, J. M. (2008). Predicting suitable habitat for the cold-water coral *Lophelia pertusa* (Scleractinia). *Deep-Sea Research Part I*, *55*(8), 1048–1062.

De Haas, H., Mienis, F., Frank, N., Richter, T. O., Steinacher, R., de Stigter, H., et al. (2009). Morphology and sedimentology of (clustered) cold-water coral mounds at the south Rockall Trough margins, NE Atlantic Ocean. *Facies*, *55*(1), 1–26.

De Mol, B., Van Rensbergen, P., Pillen, S., Van Herreweghe, K., Van Rooij, D., McDonnell, A., et al. (2002). Large deep-water coral banks in the Porcupine Basin, southwest of Ireland. *Marine Geology*, *188*(1–2), 193–231.

De Mol, L., Van Rooij, D., Pirlet, H., Greinert, J., Frank, N., Quemmerais, F., et al. (2011). Cold-water coral habitats in the Penmarc'h and Guilvinec Canyons (Bay of Biscay): Deep-water versus shallow-water settings. *Marine Geology*, *282*(1–2), 40–52.

Dorschel, B., Hebbeln, D., Rüggeberg, A., Dullo, C., & Freiwald, A. (2005). Growth and erosion of a cold-water coral covered carbonate mound in the Northeast Atlantic during the Late Pleistocene and Holocene. *Earth and Planetary Science Letters*, *233*(1–2), 33–44.

Douarin, M., Elliot, M., Noble, S. R., Sinclair, D., Henry, L.-A., Long, D., et al. (2013). Growth of north-east Atlantic cold water coral reefs and mounds during the Holocene: A high resolution U-series and 14C chronology. *Earth and Planetary Science Letters*, *375*, 176–187.

Douville, E., Sallé, E., Frank, N., Eisele, M., Pons-Branchu, E., & Ayrault, S. (2010). Rapid and precise $^{230}Th/U$ dating of ancient carbonates using Inductively Coupled Plasma-Quadrupole Mass Spectrometry. *Chemical Geology*, *272*(1–4), 1–11.

Dubois-Dauphin, Q., Colin, C., Bonneau, L., Montagna, P., Wu, Q., Van Rooij, D., et al. (2017). Fingerprinting Northeast Atlantic water masses using Neodymium isotopes. *Geochimica et Cosmochimica Acta*, *210*, 267–288.

Duineveld, G. C., Lavaleye, M. S., Bergman, M. J., De Stigter, H., & Mienis, F. (2007). Trophic structure of a cold-water coral mound community (Rockall Bank, NE Atlantic) in relation to the near-bottom particle supply and current regime. *Bulletin of Marine Science*, *81*, 449–467.

Dullo, C., Flögel, S., & Rüggeberg, A. (2008). Cold-water coral growth in relation to the hydrography of the Celtic and Nordic European continental margin. *Marine Ecology Progress Series*, *371*, 165–176.

Ellett, D. J., Edwards, A., & Bowers, R. (1986). The hydrography of the Rockall Channel—An overview. *Proceedings of the Royal Society of Edinburgh, Section B*, *88*, 61–81.

Ellett, D. J., & Martin, J. H. A. (1973). The physical and chemical oceanography of the Rockall channel. *Deep-Sea Research and Oceanography Abstracts*, *20*(7), 585–588.

Findlay, H. S., Hennige, S. J., Wicks, L. C., Navas, J. M., Woodward, E. M. S., & Roberts, J. M. (2014). Fine-scale nutrient and carbonate system dynamics around cold-water coral reefs in the northeast Atlantic. *Scientific Reports*, *4*(1), 3671 https://doi.org/10.1038/srep03671

Fink, H. G., Wienberg, C., De Pol-Holz, R., Wintersteller, P., & Hebbeln, D. (2013). Cold-water coral growth in the Alboran Sea related to high productivity during the Late Pleistocene and Holocene. *Marine Geology*, *339*, 71–82.

Frank, N., Freiwald, A., Correa, M. L., Wienberg, C., Eisele, M., Hebbeln, D., et al. (2011). Northeastern Atlantic cold-water coral reefs and climate. *Geology*, *39*(8), 743–746.

Frank, N., Paterne, M., Ayliffe, L., Van Weering, T., Henriet, J.-P., & Blamart, D. (2004). Eastern North Atlantic deep-sea corals: Tracing upper intermediate water Δ14C during the Holocene. *Earth and Planetary Science Letters*, *219*(3–4), 297–309.

Frank, N., Ricard, E., Paquet, A., van der Land, C., Colin, C., Blamart, D., et al. (2009). The Holocene occurrence of cold water corals in the NE Atlantic: Implications for coral carbonate mound evolution. *Marine Geology*, *266*(1–4), 129–142.

Frederiksen, R., Jensen, A., & Westerberg, H. (1992). The distribution of the scleractinian coral *Lophelia pertusa* around the Faeroe islands and the relation to internal tidal mixing. *Sarsia*, *77*, 157–171.

Freiwald, A. (2002). Reef-forming cold-water corals. In Wefer, G. (Ed.), *Ocean margin systems* (pp. 365–385). Berlin, Germany: Springer.

Freiwald, A., Fosså, J. H., Grehan, A., Koslow, T., & Roberts, J. M. (2004). *Cold-water coral reefs: Out of sight-no longer out of mind* (Biodiversity Series 22, 86 p.). Cambridge, UK: UNEP World Conservation Monitoring Centre.

García-Ibáñez, M. I., Pardo, P. C., Carracedo, L. I., Mercier, H., Lherminier, P., Ríos, A. F., et al. (2015). Structure, transports and transformations of the water masses in the Atlantic Subpolar Gyre. *Progress in Oceanography*, *135*, 18–36.

Hathorne, E. C., Gagnon, A., Felis, T., Adkins, J., Asami, R., Boer, W., et al. (2013). Interlaboratory study for coral Sr/Ca and other element/Ca ratio measurements. *Geochemistry, Geophysics, Geosystems*, *14*, 3730–3750. https://doi.org/10.1002/ggge.20230

Hebbeln, D., Rooij, D. V., & Wienberg, C. (2016). Good neighbours shaped by vigorous currents: Cold-water coral mounds and contourites in the North Atlantic. *Marine Geology*, *378*, 171–185.

Hillaire-Marcel, C., de Vernal, A., Bilodeau, G., & Weaver, A. J. (2001). Absence of deep-water formation in the Labrador Sea during the last interglacial period. *Nature*, *410*, 1073–1078.

Holliday, N. P., Pollard, R. T., Read, J. F., & Leach, H. (2000). Water mass properties and fluxes in the Rockall Trough, 1975 to 1998. *Deep-Sea Research Part I*, *47*(7), 1303–1332.
Hoogakker, B. A., McCave, N., Elderfield, H., Hillaire-Marcel, C., & Simstich, J. (2015). Holocene climate variability in the Labrador Sea. *Journal of the Geological Society*, *172* (2), 272–277.
Jaffey, A. H., Flynn, K. F., Glendenin, L. E., Bentley, W. C., & Essling, A. M. (1971). Precision measurements of half-lives and specific activities of $^{235}$U and $^{238}$U. *Physical Review C*, *4*(5), 1889–1906.
Kenyon, N. H., Akhmetzhanov, A. M., Wheeler, A. J., Van Weering, T. C. E., De Haas, H., & Ivanov, K. (2003). Giant carbonate mud mounds in the southern Rockall Trough. *Marine Geology*, *195*(1–4), 5–30.
Lopez Correa, M., Montagna, P., Joseph, N., Ruggeberg, A., Fietzke, J., Flogel, S., et al. (2012). Preboreal onset of cold-water coral growth beyond the Arctic Circle revealed by coupled radiocarbon and U-series dating and neodymium isotopes. *Quaternary Science Reviews*, *34*, 24–43.
Lozier, M. S., & Stewart, N. M. (2008). On the temporally-varying northward penetration of Mediterranean Overflow Water and eastward penetration of Labrador Sea Water. *Journal of Physical Oceanography*, *38*(9), 2097–2103.
Ludwig, K. R., & Titterington, D. M. (1994). Calculation of $^{230}$Th/U isochrons, ages, and errors. *Geochimica et Cosmochimica Acta*, *58*(22), 5031–5042.
Lutringer, A. (2003). *Reconstitution de la variabilité des eaux intermédiairespar l'étude de la géochimie des coraux profonds* (PhD thesis, 234 p.). Paris, France: University of Paris XI.
Masson, D. G., Bett, B. J., Billett, D. S. M., Jacobs, C. L., Wheeler, A. J., & Wynn, R. B. (2003). The origin of deep-water, coral-topped mounds in the northern Rockall Trough, Northeast Atlantic. *Marine Geology*, *194*(3–4), 159–180.
Mienis, F., De Stigter, H. C., White, M., Duineveld, G., De Haas, H., & Van Weering, T. C. E. (2007). Hydrodynamic controls on cold-water coral growth and carbonate-mound development at the SW and SE Rockall Trough Margin, NE Atlantic Ocean. *Deep-Sea Research Part I*, *54*(9), 1655–1674.
Mienis, F., van der Land, C., de Stigter, H. C., van de Vorstenbosch, M., de Haas, H., Richter, T., et al. (2009). Sediment accumulation on a cold-water carbonate mound at the Southwest Rockall Trough margin. *Marine Geology*, *265*(1–2), 40–50.
Mienis, F., Van Weering, T., De Haas, H., De Stigter, H., Huvenne, V., & Wheeler, A. (2006). Carbonate mound development at the SW Rockall Trough margin based on high resolution TOBI and seismic recording. *Marine Geology*, *233*(1–4), 1–19.
Miettinen, A., Divine, D. V., Koc, N., Godtliebsen, F., & Hall, I. R. (2012). Multicentennial variability of the sea surface temperature gradient across the subpolar North Atlantic over the last 2.8 kyr. *Journal of Climate*, *25*(12), 4205–4219.
Miettinen, A., Koç, N., Hall, I. R., Godtliebsen, F., & Divine, D. (2011). North Atlantic sea surface temperatures and their relation to the North Atlantic Oscillation during the last 230 years. *Climate Dynamics*, *36*(3–4), 533–543.
Mohn, C., Rengstorf, A., White, M., Duineveld, G., Mienis, F., Soetaert, K., et al. (2014). Linking benthic hydrodynamics and cold-water coral occurrences: A high-resolution model study at three cold-water coral provinces in the NE Atlantic. *Progress in Oceanography*, *122*, 92–104.
Montagna, P., McCulloch, M., Douville, E., López Correa, M., Trotter, J., Rodolfo-Metalpa, R., et al. (2014). Li/Mg systematics in scleractinian corals: Calibration of the thermometer. *Geochimica et Cosmochimica Acta*, *132*, 288–310.
Montero-Serrano, J.-C., Frank, N., Tisnérat-Laborde, N., Colin, C., Wu, C., Lin, K., et al. (2013). Decadal changes in the mid-depth water mass dynamic of the Northeastern Atlantic margin (Bay of Biscay). *Earth and Planetary Science Letters*, *364*, 134–144.
Moreno-Chamarro, E., Zanchettin, D., Lohmann, K., & Jungclaus, J. H. (2017). An abrupt weakening of the subpolar gyre as trigger of Little Ice Age-type episodes. *Climate Dynamics*, *48*(3–4), 727–744.
New, A. L., & Smythe-Wright, D. (2001). Aspects of the circulation in the Rockall Trough. *Continental Shelf Research*, *21*(8–10), 777–810.
O'Brien, S. R., Mayewski, P. A., Meeker, L. D., Meese, D. A., Twickler, M. S., & Whitlow, S. I. (1995). Complexity of Holocene climate as reconstructed from a Greenland ice core. *Science*, *270*(5244), 1962–1964.
Pirlet, H., Colin, C., Thierens, M., Latruwe, K., Van Rooij, D., Foubert, A., et al. (2011). The importance of the terrigenous fraction within a cold-water coral mound: A case study. *Marine Geology*, *282*(1–2), 13–25.
Pollard, R. T., Griffttths, M. J., Cunningham, S. A., Read, J. F., Pérez, F. F., & Ríos, A. F. (1996). Vivaldi 1991—A study of the formation, circulation and ventilation of Eastern North Atlantic Central Water. *Progress in Oceanography*, *37*(2), 167–172.
Pons-Branchu, E., Douville, E., Roy-Barman, M., Dumont, E., Branchu, P., Thil, F., et al. (2014). A geochemical perspective on Parisian urban history based on U-Th dating, laminae counting and yttrium and REE concentrations of recent carbonates in underground aqueducts. *Quaternary Geochronology*, *24*, 44–53.
Pons-Branchu, E., Hillaire-Marcel, C., Ghaleb, B., Deschamps, P., & Sinclair, D. (2005). Early diagenesis impact on precise U-series dating of Deep-Sea corals. Example of a 100–200 years old *Lophelia pertusa* sample from NE Atlantic. *Geochimica et Cosmochimica Acta*, *69*(20), 4865–4879.
Raddatz, J., Rüggeberg, A., Liebetrau, V., Foubert, A., Hathorne, E. C., Fietzke, J., et al. (2014). Environmental boundary conditions of cold-water coral mound growth over the last 3 million years in the Porcupine Seabight, Northeast Atlantic. *Deep-Sea Research Part II*, *99*, 227–236.
Raddatz, J., Ruggeberg, A., Margreth, S., Dullo, W. C., & Party, I. E. S. (2011). Paleoenvironmental reconstruction of Challenger Mound initiation in the Porcupine Seabight, NE Atlantic. *Marine Geology*, *282*(1–2), 79–90.
Reimer, P. J., Bard, E., Bayliss, A., Beck, J. W., Blackwell, P. G., Bronk Ramsey, C., et al. (2013). Intcal13 and Marine13 radiocarbon age calibration curves 0-50,000 years cal BP. *Radiocarbon*, *55*(4), 1869–1887.
Roberts, J. M., Davies, A. J., Henry, L. A., Dodds, L. A., Duineveld, G. C. A., Lavaleye, M. S. S., et al. (2009). Mingulay reef complex: An interdisciplinary study of cold-water coral habitat, hydrography and biodiversity. *Marine Ecology Progress Series*, *397*, 139–151.
Rüggeberg, A., Flögel, S., Dullo, W. C., Raddatz, J., & Liebetrau, V. (2016). Paleo-seawater density reconstruction and its implication for cold-water coral carbonate mounds in the northeast Atlantic through time. *Paleoceanography*, *31*, 365–379. https://doi.org/10.1002/2015PA002859
Sánchez, F., González-Pola, C., Druet, M., García-Alegre, A., Acosta, J., Cristobo, J., et al. (2014). Habitat characterization of deep-water coral reefs in La Gaviera Canyon (Avilés Canyon System, Cantabrian Sea). *Deep-Sea Research Part II*, *106*, 118–140.
Schröder-Ritzau, A., Freiwald, A., & Mangini, A. (2005). U/Th-dating of deep-water corals from the eastern North Atlantic and the western Mediterranean Sea. In Freiwald, A. & Roberts, J. M. (Eds.), *Cold-water corals and ecosystems* (pp. 1151–1169). Berlin, Germany: Springer.
Solignac, S., de Vernal, A., & Hillaire-Marcel, C. (2004). Holocene sea-surface conditions in the North Atlantic—Contrasted trends and regimes in the western and eastern sectors (Labrador Sea vs. Iceland Basin). *Quaternary Science Reviews*, *23*(3–4), 319–334.
Somoza, L., Ercilla, G., Urgorri, V., León, R., Medialdea, T., Paredes, M., et al. (2014). Detection and mapping of cold-water coral mounds and living *Lophelia* reefs in the Galicia Bank, Atlantic NW Iberia margin. *Marine Geology*, *349*, 73–90.

Sorrel, P., Debret, M., Billeaud, I., Jaccard, S. L., McManus, J. F., & Tessier, B. (2012). Persistent non-solar forcing of Holocene storm dynamics in coastal sedimentary archives. *Nature Geoscience*, *5*(12), 892–896.

Thierens, M., Pirlet, H., Colin, C., Latruwe, K., Vanhaecke, F., Stuut, J.-B., et al. (2012). Evidence for an ice-rafting British-Irish ice sheet since the earliest Pleistocene (2.6 million years ago)): Early mid-latitudinal glaciation around the North Atlantic Ocean. *Quaternary Science Reviews*, *44*, 229–240.

Thornalley, D. J., Elderfield, H., & McCave, N. (2009). Holocene oscillations in temperature and salinity of the surface subpolar North Atlantic. *Nature*, *457*(7230), 711–714.

Tisnérat-Laborde, N., Poupeau, J. J., Tannau, J. F., & Paterne, M. (2001). Development of a semi-automated system for routine preparation of carbonate samples. *Radiocarbon*, *43*(2A), 299–304.

van der Land, C., Eisele, M., Mienis, F., de Haas, H., Hebbeln, D., Reijmer, J. J. G., et al. (2014). Carbonate mound development in contrasting settings on the Irish margin. *Deep-Sea Research Part I*, *99*, 297–306.

Van der Land, C., Mienis, F., De Haas, H., Frank, N., Swennen, R., & Van Weering, T. (2010). Diagenetic processes in carbonate mound sediments at the southwest Rockall Trough margin. *Sedimentology*, *371*, 165–176.

van Haren, H., Mienis, F., Duineveld, G. C., & Lavaleye, M. S. (2014). High-resolution temperature observations of a trapped nonlinear diurnal tide influencing cold-water corals on the Logachev mounds. *Progress in Oceanography*, *125*, 16–25.

Van Weering, T. C. E., De Haas, H., De Stigter, H. C., Lykke-Andersen, H., & Kouvaev, I. (2003). Structure and development of giant carbonate mounds at the SW and SE Rockall Trough margins, NE Atlantic Ocean. *Marine Geology*, *198*(1–2), 67–81.

Van Weering, T. C. E., Dullo, C., & Henriet, J.-P. (2003). An introduction to geosphere-biosphere coupling: Cold seep related carbonate and mound formation and ecology. *Marine Geology*, *198*(1–2), 1–3.

Victorero, L., Blamart, D., Pons-Branchu, E., Mavrogordato, M. N., & Huvenne, V. A. I. (2016). Reconstruction of the formation history of the Darwin Mounds, N Rockall Trough: How the dynamics of a sandy contourite affected cold-water coral growth. *Marine Geology*, *378*, 186–195.

Wade, I. P., Ellett, D. J., & Heywood, K. J. (1997). The influence of intermediate waters on the stability of the eastern North Atlantic. *Deep-Sea Research Part I*, *44*(8), 1405–1426.

White, M., & Dorschel, B. (2010). The importance of the permanent thermocline to the cold water coral carbonate mound distribution in the NE Atlantic. *Earth and Planetary Science Letters*, *296*(3–4), 395–402.

White, M., Mohn, C., de Stigter, H., & Mottram, G. (2005). Deep water coral development as a function of hydrodynamics and surface productivity around the submarine banks of the Rockall Trough, NE Atlantic. In Freiwald, A. & Roberts, J. M. (Eds.), *Cold water corals and ecosystems* (pp. 503–514). Berlin, Germany: Springer.

Wienberg, C., Frank, N., Mertens, K. N., Stuut, J.-S., Marchant, M., Fietzke, J., et al. (2010). Glacial cold-water coral growth in the Gulf of Cádiz: Implications of increased palaeo-productivity. *Earth and Planetary Science Letters*, *298*(3–4), 405–416.